# Improving the efficiency of wide-angle seismic data inversion through a nonlinear algorithm: case study of the MARCONI-3 profile

***Mejorando la eficiencia de la inversión de datos de sísmica de gran ángulo por medio de un algoritmo no lineal: aplicación al perfil MARCONI-3***

**Andrés Olivar-Castaño[1], Irene DeFelipe[2], Marco Pilz[3], Mario Ruiz[4] and Ramón Carbonell[4]**

1 Departamento de Geología, Universidad de Oviedo. C/Jesús Arias de Velasco s/n, 33005 Oviedo, Asturias, olivar@geol.uniovi.es
2 Departamento de Geología, Universidad de Salamanca, Plaza de la Merced, s/n, 37008, Salamanca, idefelipe@usal.es
3 Helmholtz-Zentrum Potsdam – GeoForschungsZentrum (GFZ). Telegrafenberg, 14467, Potsdam, Alemania, pilz@gfz-potsdam.de
4 Instituto Geociencias Barcelona, Lluis Solé Sabaris s/n 08028 Barcelona GEO3BCN-CSIC, mruiz@geo3bcn.csic.es, rcarbo@geo3bcn.csic.es

**ABSTRACT**

*Wide-angle seismic reflection/refraction (WA) surveys provide data that can be modeled to obtain lithospheric-scale P-wave velocity (VP) models. The interpretation of these datasets is often performed as a laborious and time-consuming trial-and-error procedure, in which the relevant model parameters (layer thickness and VP) are manually adjusted until the forward modeling matches the observed travel-times. In this work, we present a fully automatic iterative nonlinear approach to invert WA datasets based on the simulated annealing technique. We test our proposed approach with data from the MARCONI-3 WA profile (southern Bay of Biscay) and compare the outcome with an existing detailed interpretation, discussing the similarities between the two models and the agreement between our model and the observed travel-times.*

**Key-words**: *simulated annealing, nonlinear inversion, wide-angle seismics, crustal structure.*

**RESUMEN**

*Los estudios de reflexión/refracción sísmica de gran ángulo (WA) proporcionan datos que se pueden invertir para obtener modelos de velocidad de ondas P (VP) a escala litosférica. La interpretación de este tipo de datos se realiza a menudo a través de un laborioso procedimiento de prueba y error que puede requerir mucho tiempo, en el que los parámetros relevantes del modelo (espesor de las capas y VP) se ajustan manualmente hasta que la modelización directa se ajusta a los tiempos de llegada observados. En este trabajo, presentamos un enfoque no lineal iterativo totalmente automático para la inversión de datos de WA basado en la técnica de enfriamiento simulado. Probamos nuestro enfoque propuesto con datos del perfil MARCONI-3 WA (al sur del Golfo de Vizcaya) y comparamos el resultado con una interpretación detallada ya existente, discutiendo las similitudes entre los dos modelos y la concordancia entre nuestro modelo y los tiempos de llegada observados.*

**Palabras clave:** *enfriamiento simulado, inversión no lineal, sísmica de gran ángulo, estructura cortical*

*Geogaceta, 71 (2022), 27-30*
*ISSN (versión impresa): 0213-683X*
*ISSN (Internet): 2173-6545*

*Fecha de recepción: 28/07/2021*
*Fecha de revisión: 29/10/2021*
*Fecha de aceptación: 26/11/2021*

## Introduction

Wide-angle seismic reflection/ refraction (WA) data provide very valuable information about the seismic P-wave velocity ($V_p$) distribution in the crust and upper mantle, as well as the depth of major lithospheric discontinuities. One of the most common approaches to retrieve a $V_p$ model from a WA dataset involves manually editing the model parameters ($V_p$ distribution and layer thickness) and computing synthetic travel-times using a ray-tracing algorithm. The predicted travel-times are then visually inspected and compared with the ones observed in the WA survey, and the whole process is repeated until a sufficient match is found. This manual trial-and-error approach has the important advantage of allowing the interpreter to impose detailed constraints upon the $V_p$ model based on their geological knowledge of the study area. However, it also has several disadvantages. First, the task can be very time consuming. Second, obtaining a good fit to the observed travel-times can prove to be very difficult (especially when considering multiple active sources at the same time, some of which might not even be in the same plane as the seismic line). Third, this technique does not rely on any quantitative measurement of the quality of the fit between the observed and predicted travel-times. Finally, although it is not strictly a disadvantage, the trial-and-error procedure may not provide the interpreter with a sense of the non-uniqueness that affects the inverse problem. To avoid these issues, a number of inversion algorithms have been developed over the years (Zelt, 1999). Although a few nonlinear applications exist (e.g., Pica et al., 1990), most of these algorithms linearize the traveltime inversion problem around an initial model, and then use iterative-least squares techniques to update the model with the aim of minimizing a certain objetive funcion (e.g., the error between the observed and predicted travel-times). The main advantage of linearized approaches is that they are fast (usually requiring only a few iterations). However, a poor choice of an initial model may cause these algorithms to get stuck in a local minimum of the objetive function, which prevents further improvements to the model. In contrast, while usually requiring many more iterations and thus more computing time, nonlinear algorithms can provide a much more complete exploration of the model space, which makes them far less vulnerable to the local minima problem and thus

much more capable of finding the best-fitting model. For this reason, nonlinear algorithms are well-suited for solving complex combinatorial problems, such as choosing the correct distribution of $V_P$ to match the observed WA travel-times.

## Simulated annealing algorithm for the inversion of WA data

In this contribution, we present a nonlinear approach for the inversion of WA data based on the simulated annealing technique (Kirkpatrick et al., 1983). Simulated annealing is an optimization method that uses a combination of random and directed search methods to efficiently sample the model space. The algorithm is controled by two parameters: i) the misfit or objective function (*E*), which provides a quantitative measurement of the quality of a given solution, and ii) the temperature (*T*) which decreases each iteration according to a certain cooling schedule that must be chosen by the user. The algorithm starts from an initial solution and then searches the model space for new solutions. New solutions are accepted or rejected based on the values of *E* and *T*. If the misfit *E* of a proposed model is smaller than that of the current model, the new model is always accepted. However, the new model can also be accepted even if the misfit *E* increases, according to the Metropolis-Hastings rule (Metropolis et al., 1953):

$$p(m)\alpha\, exp\left(\frac{-\Delta E(m)}{T}\right), \qquad (1)$$

where $\alpha$ indicates proportionality, *p(m)* is the acceptance probability of the new model *m*, *ΔE(m)* is the difference between the misfit of the current model and the new model, and T is the value of the temperature at the current iteration. When *T* is large at the beginning of the inversion, new solutions are frequently accepted, which translates into a random search of the model space. As the iterations continue and *T* becomes progressively smaller, decreases in the objective function *E* are favored, and the search for new models becomes increasingly directed. The capability of sometimes accepting worse models is the most important property of the simulated annealing technique, as it allows the algorithm to avoid getting stuck in local minima of the objective function.

The cooling schedule of the simulated annealing algorithm comprises the initial temperature, the temperature decrease rule, and the number of iterations that are performed between two consecutive temperature decreases (the so-called equilibrium condition). These parameters are all closely linked to the objective function and the parametrization of the model. In this study, we have chosen to compute the error of the trial models as the norm of the difference between two matrices containing the observed and predicted travel-times. In this way, we can estimate the misfit without the need to identify the different P-wave phase arrivals. To select the initial temperature, we have followed the iterative method described by Ben-Ameur (2004). For the temperature decrease we have chosen the commonly used geometric rule, , where $\beta$ is a number close to but less than 1 (Kirkpatrick et al., 1983). Finally, we have chosen the number of iterations between consecutive temperature decreases to be equal to the number of model parameters (Kirkpatrick, 1984).

In our approach, the forward computations were carried out by the RAYINVR package (Zelt & Smith, 1992). This code was chosen because it provides a very flexible parametrization of the $V_P$ models, consisting on a series of nodes that represent the geometry of the layers and the distribution of $V_P$. New models are generated by randomly selecting a geometry and a $V_P$ node, and then applying a variation drawn from a normal probability distribution centered in the original value.

We have tested our proposed inversion procedure with traveltime data from three ocean bottom seismometers located in the offshore section of profile 3 of the MARCONI-WA project (Fig. 1). This dataset provides a great oportunity to test our algorithm, as a previous $V_P$ forward model exists (Ruiz et al., 2017).

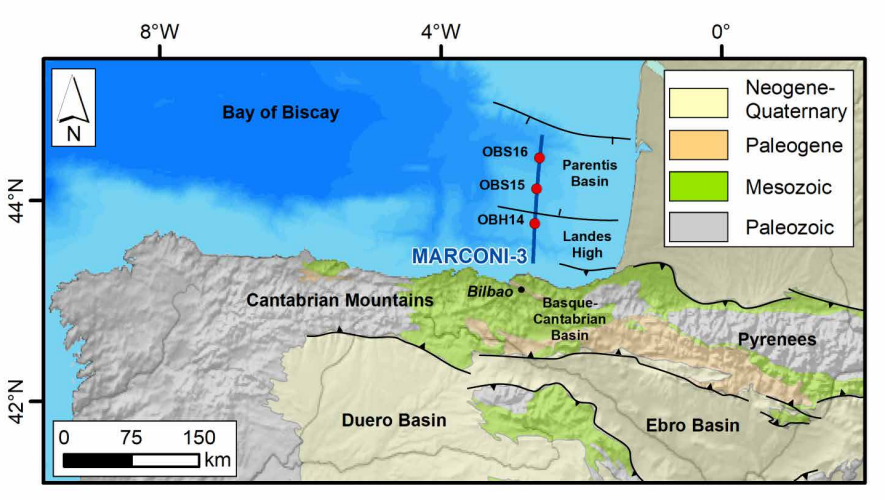


**Fig. 1. Location of the MARCONI-3 profile (blue line) in the southern Bay of Biscay. Ver figura en color en la web.**
***Fig. 1. Situación del perfil MARCONI-3 (línea azul) al sureste del golfo de Vizcaya. See color figure in the web.***

## Geological setting

The MARCONI-WA data acquisition was carried out in the southeastern sector of the Bay of Biscay and consisted of 11 profiles (Ruiz, 2007; Ruiz et al. 2017). Within this project, profile 3 runs for 240 km in a N-S direction, sampling the northernmost part of the Basque-Cantabrian Basin and crossing the Landes High and Parentis Basin offshore (Figure 1). This seismic survey was aimed at improving the knowledge over the tectonic evolution of the region during Mesozoic and Cenozoic times, the kinematics of the Iberian subplate, and the exhumation of a Cretaceous hyperextended rift system (e.g. Ferrer et al. 2008; Roca et al., 2011; Ruiz et al. 2017; Cadenas et al. 2018). During the opening of the Biscay Bay in Cretaceous times, this area was subjected to a hyperextension process that stretched the crust and caused mantle exhumation towards the eastern Basque-Cantabrian Basin (DeFelipe et al., 2017) and the central part of the Bay of Biscay, as well as the development of hyperthinned crustal domains towards the eastern Bay of Biscay (Roca et al., 2011; Tugend et al., 2014). In the context of the Alpine orogeny during Cenozoic times, the tectonic inversion closed partially the Bay of Biscay, exhumed the Pyrenees and the Cantabrian Mountains, deformed the North Iberian Margin, promoted the

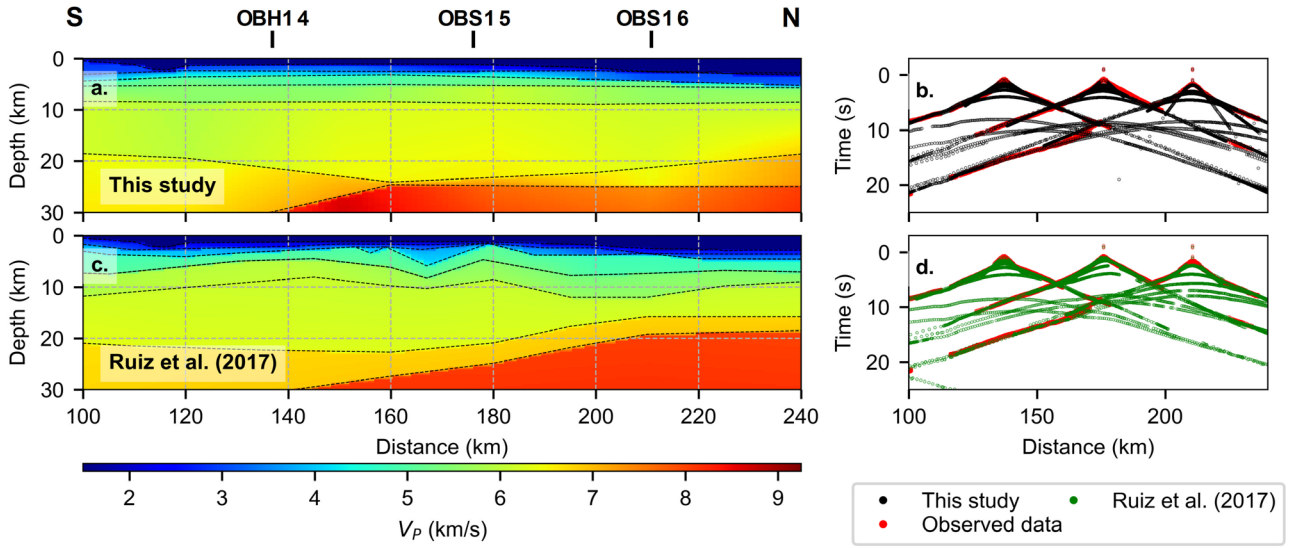


**Fig. 2. (a) VP model obtained in this work for the offshore part of the MARCONI-3 profile. (b) Predicted travel-times using the rayinvr package (Zelt & Smith, 1992) for the model in (a). (c) Trial-and-error VP model by Ruiz et al. (2017). (d) Predicted travel-times for the model by Ruiz et al. (2017). Ver figura en color en la web.**

***Fig. 2. (a) Perfil de VP obtenido en este trabajo para la parte offshore del perfil MARCONI-3. (b) Tiempos de llegada estimados para el modelo mostrado en (a) utilizando el programa rayinvr (Zelt y Smith, 1992). (c) Modelo obtenido por Ruiz et al. (2017) (d) Tiempos de llegada estimados para el modelo de Ruiz et al. (2017). See color figure in the web.***

northwards subduction of the Iberian subplate under the European plate (Pedreira et al., 2003; 2007; Ruiz et al., 2017; DeFelipe et al., 2018; 2019) and the southward subduction of the oceanic crust of the Bay of Biscay (e.g., Teixell et al., 2018). This tectonic configuration resulted in a complex indentation of the Iberian and European plates that has been imaged by different WA surveys (Pedreira et al., 2003; Ruiz et al., 2017), potential field modeling (Pedreira et al., 2007) and seismic ambient noise tomography (Olivar-Castaño et al., 2020). Towards the north of the inverted Basque-Cantabrian Basin, the Landes High acted as a buffer for the propagation of the contractional deformation (Ferrer et al., 2008).

## Results

The initial model used in the nonlinear inversion was a simple stack of 6 laterally homogeneous layers, with $V_P$ velocities increasing with depth. For each layer, velocity and geometry nodes were placed every 30 km and 40 km, respectively. This excludes layer 1 (representing the sea water) and the geometry of layer 2 (the ocean floor), which in any case were not modified during the nonlinear inversion. The reason behind the relatively simple parametrization was to avoid the overfitting of the observed travel-times. The inversion procedure did not allow $V_P$ inversions.

The results are summarized in Fig. 2. Fig. 2a shows the best-fitting model obtained during the inversion, and Fig. 2b shows the observed and predicted travel-times for comparison. Fig. 2c contains the offshore part of the model previously obtained by Ruiz et al. (2017) for the complete profile 3 dataset using the manual trial-and-error procedure and including additional normal incidence and gravity constraints (Ferrer et al., 2008). Fig. 2d shows the fit of their predicted travel-times for the three OBSs considered in this study.

Overall, the predicted travel-times fit well the observed ones (Fig. 2b). The RMS (root mean square) error for our model is 0.667 s, higher than the value reported for the model by Ruiz et al. (2017), 0.192 s. The increased RMS for our model is likely related to the coarse parametrization of the $V_P$ and geometry nodes. Crustal thickness is poorly constrained by our dataset due to the lack of Pn and PmP arrivals, with the only records of the PmP phase being provided by OBS16 in the ~110-180 km range. However, these arrivals are not enough to constraint the geometry of the lower crust or the Moho. Therefore, we do not interpret the model below 20 km. High $V_P$ values were retrieved at a relatively shallow depth (15-20 km) in the northern part of the profile, which could be coherent with the crustal thinning observed by Ruiz et al. (2017). Closer to the surface, the $V_P$ distribution resembles that of Ruiz et al. (2017), with a noticeable velocity contrast located at a depth of ~10 km. It is worth noting that both models fit reasonably well the observed dataset, even though the one by Ruiz et al. (2017) includes many more constraints and thus is better resolved. This evidences the non-uniqueness that affects the travel-time inversion problem.

## Discussion

The simulated annealing procedure allows for a more purposeful search for the best-fitting $V_P$ model. Even though only one constraint was placed upon the inversion (i.e., $V_P$ is only allowed to increase with increasing depth), the best-fitting $V_P$ model obtained is coherent in a broad sense with both the geological knowledge of the area and a previous interpretation of the same dataset using a forward modeling approach. The computation time required for our proposed inversion scheme depends heavily on the performance of the ray-tracing algorithm (in the case of RAYINVR, performance depends on the complexity of the model parametrization and the number of rays to be traced) and is usually in the range of a few hours. The inversion can be stopped when the ratio of acceptance of new models falls below a certain threshold (e.g., 5%).

The results produced by the algo-

rithm could be improved by adding more geological information in the form of additional constraints, as it has been shown that adequate constraints can dramatically improve the performance and reduce the computational effort of any nonlinear inversion by reducing the non-uniqueness of the problem (e.g., Sambridge, 2001). For instance, for our application example, further constraints could be implemented according to the interpretation of the normal incidence seismic reflection survey presented by Ferrer et al. (2008). Nevertheless, we wanted to test the performance of the algorithm using the least amount of a priori information possible. Spatial resolution (and therefore the fit to the observed travel-times) could be further improved by adding more geometry and/or $V_P$ nodes to the initial model. In that case, a smoothing constraint should be added to prevent overfitting.

## Conclusions

We have presented a simulated annealing algorithm for the inversion of WA datasets. In our approach, the forward computations are taken care of by the popular RAYINVR package (Zelt & Smith, 1992). The capabilities of the inversion algorithm were tested using data recorded by three ocean bottom seismometers deployed in the southeastern sector of the Biscay Bay for the acquisition of profile 3 of the MARCONI-WA project. Our results show that the simulated annealing algorithm can recover a $V_P$ velocity model that fits well the observed travel-times. The $V_P$ model is coherent with the results of the forward modeling presented by Ruiz et al. (2017). In contrast to the manual forward modeling method, user intervention is only required to provide an initial model and to select a cooling schedule. Future lines of work include making improvements to the model parametrization in order to obtain smoother and better resolved models, and to the objective function, which will increase the effectiveness of the algorithm in the search of the model space.

## Data availability

The MARCONI-WA dataset (Gallart et al., 2020) is available in the Seismic DAta REpository, SeisDARE (DeFelipe et al., 2021).

## Acknowledgements

We would like to thank two anonymous reviewers for their helpful comments, which improved the quality of this manuscript.

## References

Ben-Ameur, W. (2004). *Computational Optimization and Applications, 29*, 369-385.

Cadenas, P., Fernández-Viejo, G., Pulgar, J. A., Tugend, J., Manatschal, G. and Minshull, T. A. (2018). T*ectonics, 37*(3), 758–785, doi: 10.1002/2016TC004454

DeFelipe, I., Pedreira, D., Pulgar, J. A., Iriarte, E. and Mendia, M. (2017). *Geochemistry, Geophysics, Geosystems, 18*(2), doi: 10.1002/2016GC006690

DeFelipe, I., Pulgar, J. A. and Pedreira, D. (2018). *Revista de la Sociedad Geológica de España, 31*(2), 69–82. doi: 10.13039/501100003329

DeFelipe, I., Pedreira, D., Pulgar, J. A., van der Beek, P. A., Bernet, M. and Pik, R. (2019). *Tectonics, 38*(9), 3436–3461, doi: 10.1029/2019TC005532

DeFelipe, I., Alcalde, J., Ivandic, M., Martí, D., Ruiz, M., Marzán, I. et al. (2021). *Earth System Science Data, 13*, 1053–1071, doi: 10.5194/essd-13-1053-2021

Ferrer, O., Roca, E., Benjumea, B., Muñoz, J. A., Ellouz, N., Gallart, J., et al. (2008). *Marine and Petroleum Geology, 25*(8), 714–730, doi: 10.1016/j.marpetgeo.2008.06.002

Gallart, J., Pulgar, J. A., Muñoz, J. A., Diaz, J., and Ruiz, M. (2020). *DIGITAL.CSIC, doi: 10.20350/digitalCSIC/12685.*

Kirkpatrick, S. (1984). J*ournal of Statistical Physics, 34*, pages 975–986.

Kirkpatrick, S., Gelatt, C. D., Vecchi, M. P. (1983). *Science, 220*, 4598, 671-680.

Metropolis, N., Rosenbluth, W. A., Rosenbluth, M. N. and Teller, A. H. (1953). J*ournal of Chemical Physics, 21*(6), 1087-1092

Olivar-Castaño, A., Pilz, M., Pedreira, D., Pulgar, J. A., Díaz-González, A., and González-Cortina, J. M. (2020). *Journal of Geophysical Research: Solid Earth, 125,* 1–20, doi: 10.1029/2020JB019559

Pedreira, D., Pulgar, J. A., Gallart, J., and Díaz, J. (2003). *Journal of Geophysical Research: Solid Earth, 108*(B4), 1–21, doi: 10.1029/2001jb001667

Pedreira, D., Pulgar, J. A. and Torné, M. (2007). *Journal of Geophysical Research: Solid Earth, 112*(B12), doi: 10.1029/2007JB005021

Pica, A., Diet, J. P., Tarantola, A. (1990). *Geophysics, 55*, 3, 266-379.

Roca, E., Muñoz, J. A., Ferrer, O., and Ellouz, N. (2011). *Tectonics, 30*(2), 1–33, doi: 10.1029/2010TC002735

Ruiz, M. (2007). *Caracterització estructural i sismotectònica de la litosfera en el domini Pirenaico-Cantàbric a partir de mètodes de sísmica activa i passiva*. PhD Thesis, Universitat de Barcelona.

Ruiz, M., Díaz, J., Pedreira, D., Gallart, J., and Pulgar, J. A. (2017). *Tectonophysics, 717,* 65–82, doi: 10.1016/j.tecto.2017.07.008

Sambridge, M. (2001). *Inverse Problems, 17*, 387–403.

Teixell, A., Labaume, P., Ayarza, P., Espurt, N., de Saint Blanquat, M. and Lagabrielle, Y. (2018). *Tectonophysics, 724-725,* 146-170. doi: 10.1016/j.tecto.2018.01.00

Tugend, J., Manatschal, G., Kusznir, N. J., Masini, E., Mohn, G., and Thinon, I. (2014). *Tectonics, 33*(7), 1239–1276, doi: 10.1002/2014TC003529

Zelt, C. (1999). *Geophysical Journal International 139*(1), 183-204.

Zelt, C., and Smith, R. (1992). *Geophysical Journal International, 108*(1), 16 – 34.